PNAS
www.pnas.org

Main Manuscript for

The influence of iodine on the Antarctic stratospheric ozone hole

Carlos A. Cuevas[1,*], Rafael P. Fernandez[2-3], Douglas E. Kinnison[4], Qinyi Li[1], Jean-François Lamarque[5], Tarek Travelsi[6], Joseph S. Francisco[6], Susan Solomon[7], and Alfonso Saiz-Lopez[1,*]

[1]Department of Atmospheric Chemistry and Climate, Institute of Physical Chemistry Rocasolano, CSIC, Madrid, 28006, Spain

[2]Institute for Interdisciplinary Science, National Research Council (ICB-CONICET), Mendoza, 5501, Argentina

[3]School of Natural Sciences, National University of Cuyo (FCEN-UNCuyo), Mendoza, 5501, Argentina

[4]Atmospheric Chemistry Observation and Modeling, National Center for Atmospheric Research, Boulder, CO 80305, USA

[5]Climate and Global Dynamics Laboratory, National Center for Atmospheric Research, Boulder, CO 80305, USA

[6]Department of Chemistry, University of Pennsylvania, Philadelphia, PA 19104, USA

[7]Department of Earth, Atmospheric, and Planetary Sciences, Massachusetts Institute of Technology, Cambridge, MA, 02139, USA

*Corresponding author: Alfonso Saiz-Lopez and Carlos A. Cuevas

Email: a.saiz@csic.es; ccuevas@iqfr.csic.es

Author Contributions

A.S.-L. designed research. C.A.C. and R.P.F. with the help of D.E.K., conducted WACCM model development and simulations. C.A.C., R.P.F. and A.S.-L., with significant contributions from D.E.K., Q.L., J.F.-L., S.S., evaluated and analyzed the model results. T.T. and J.S.F. conducted the ab-initio computations on iodate photochemistry. C.A.C. and A.S.-L. wrote the manuscript with contributions from all authors.

Competing Interest Statement

The authors declare no competing interests.

Classification:

PHYSICAL SCIENCES: Earth, Atmospheric, and Planetary Sciences

Keywords

Iodine, ozone depletion, Antarctic ozone hole, halogens

This PDF file includes:

Main Text
Figures 1 to 6
Tables 1 to 1

Abstract

The catalytic depletion of Antarctic stratospheric ozone is linked to anthropogenic emissions of chlorine and bromine. Despite its larger ozone-depleting efficiency, the contribution of ocean-emitted iodine to ozone hole chemistry has not been evaluated, due to the negligible iodine levels previously reported to reach the stratosphere. Based on the recently observed range (0.77±0.1 parts per trillion by volume, pptv) of stratospheric iodine injection, we use the chemistry-climate model WACCM to assess for the first time the role of iodine on the formation and recent past evolution of the Antarctic ozone hole. Our 1980-2015 simulations indicate that iodine can significantly impact on the lower edge of the Antarctic ozone hole, contributing on average 11% of the lower stratospheric ozone loss during spring (up to 4.2% of the total stratospheric column). We find that the inclusion of iodine advances the beginning and delays the closure stages of the ozone hole by 3-5 days, increasing its area and mass deficit by 11% and 20%, respectively. Despite being present in much smaller amounts, and due to faster gas-phase photochemical reactivation, iodine can dominate (~65%) the halogen-mediated ozone loss during summer and early fall, when the heterogeneous reactivation of inorganic chlorine and bromine reservoirs is reduced. The ozone destruction caused by 0.77 pptv of iodine is equivalent to that of 2.8 (4.4) pptv of biogenic very-short lived bromocarbons during spring (rest of sunlit period). Anthropogenic ozone pollution has increased ocean iodine emissions in the past decades and it is projected to continue increasing. Consequently, the relative contribution of iodine to future stratospheric ozone loss is likely to increase as anthropogenic chlorine and bromine emissions decline following the Montreal Protocol.

Significance Statement

The role of chlorine and bromine in Antarctic stratospheric ozone depletion is well known. However, the contribution of iodine to the ozone hole chemistry has not been assessed, mainly due to the negligible amounts of iodine previously reported to enter the stratosphere. New measurements demonstrate that the injection of iodine to the lower stratosphere is higher than previously assumed. Based on these observations, our modelling work shows that iodine chemistry can enhance spring ozone loss at the lower edge of the Antarctic ozone hole, and even dominate the halogen-mediated ozone loss during summer. Iodine can also alter by several days the timing of the seasonal formation and closure of the ozone hole, Therefore, models need to include iodine chemistry to fully estimate ozone depletion in the Antarctic stratosphere.

Main Text

The role played by chlorine atoms on the catalytic destruction of stratospheric ozone, after the photolytic dissociation of chlorofluorocarbons emitted by anthropogenic activities, was proposed by Molina and Rowland in the 1970s (1). The decrease in the stratospheric ozone column density in early spring over Antarctica was discovered in 1985 by Farman et al., (2). Further use of satellite measurements (3) defined the region in which stratospheric ozone was highly depleted. Simultaneous ground-based measurements of stratospheric ClO, HCl, $ClONO_2$ and OClO over Antarctica during springtime in 1986 (4–6) determined the key role of active chlorine chemistry on ozone hole formation. This was confirmed by the remarkable anticorrelation in the time evolution of observed high ClO levels and the strong ozone depletion reported by aircraft observations in the lower stratosphere (7). Bromine was also identified to participate in the catalytic cycling of stratospheric ozone destruction through the coupling with chlorine radicals (8, 9). Most of the stratospheric bromine comes from anthropogenic emissions of long-lived sources such as halons (10, 11), although biogenic very-short lived substances (VSLS) naturally emitted from the ocean also contribute ~25% to the stratospheric bromine burden (11–16).

In the 1990s, Solomon et al., already speculated that if 1 pptv (parts per trillion by volume) of iodine was injected to the stratosphere, iodine chemistry could be a contributing factor in widespread ozone depletion in the lower stratosphere (17). However, subsequent observational work suggested that the total amount of iodine entering the stratosphere was estimated to be less than 0.15 pptv (18–22), which was considered to have a negligible role in stratospheric ozone photochemistry (23). Recent modelling work based on novel tropospheric profile observations of iodine oxide (IO) suggested that the levels of iodine injected to the stratosphere were more likely to be ~0.7 pptv (24). More recently, direct measurements of IO and particulate iodine in the upper troposphere and lower stratosphere, in combination with models, have indeed confirmed that 0.77±0.10 pptv of total inorganic iodine enters the stratosphere via tropical convective outflow (25). Even though there are still uncertainties regarding the processes controlling iodine gas-to-particle partitioning during reactive transport to the stratosphere (25), the contribution of the observed stratospheric iodine injection to ozone loss within the Antarctic ozone hole remains unknown. Much of the available iodine is thought to be of natural origin, and iodine can affect stratospheric ozone in the pre-anthropogenic atmosphere (particularly via photolysis of OIO, reaction of IO with HO_2, or the reaction of IO with natural BrO). Iodine can also deplete stratospheric ozone as chlorine and bromine increase due to anthropogenic perturbations in ClO and BrO, due to what are referred to here as inter-halogen reactions (i.e., IO+ClO and IO+BrO). In this paper, we evaluate the overall effect of iodine on Antarctic stratospheric ozone and do not explicitly separate the portion affected by anthropogenic activity.

We use the specified dynamics version of the Whole Atmosphere Community Climate Model, version 4 (WACCM4-SD) (26–29), to assess the currently neglected role played by iodine chemistry on the formation and evolution of the stratospheric ozone hole between 1980 and 2015, based on the recently measured range of stratospheric iodine injection (24, 25). The model is updated with a state-of-the-art scheme of the atmospheric chemistry of halogens from the earth's surface to the stratopause (30–32), reproducing the recently measured range of stratospheric iodine injection (24, 25). We find that the contribution of iodine to ozone destruction can be up to 18% at 140 hPa during the Antarctic spring in the region 90ºS-70ºS, with a maximum decrease of ~4.2% in the stratospheric ozone column. Notably, the inclusion of iodine sources and chemistry advances the initial formation and delays the closure stages of the Antarctic ozone hole seasonal cycle. Our model results also reveal that during the austral summer and fall, iodine prevails as the dominant (~65%) halogen-driven ozone destruction chemistry in the Antarctic stratosphere.

Iodine transport to the stratosphere and gas-to-particle partitioning

Recent aircraft observations supported by a global model reported that 0.77 ± 0.10 pptv of total inorganic iodine (I_y; see definition in Methods) are currently being injected to the stratosphere, of which ~0.21 pptv (27 %) are in the gas-phase, and ~0.56 pptv (73 %) are bound to aerosols, mainly as iodate (25). The heterogeneous ultraviolet (UV) photolysis of iodate releasing reactive iodine to the gas phase has been demonstrated in laboratory studies (33, 34). We have also conducted theoretical calculations to define the energy thresholds for the photo-fragmentation from iodate particles back to gas-phase iodine (Supplementary Information). The potential energy surface (PES) of IO_3^- is characterized by many excited states that are stable and display minima in their PES (their minimum located below the ground state of the neutral and correlated to dissociation limits located below the first dissociation limit of the neutral) (Fig S1). The absorption of a photon in the visible or near UV region i.e. ($263 < h\nu < 442$ nm) exciting these states may lead to the production of IO_2^-+O or IO_2+O^-. Indeed, there are three triplet states that correlate to the first dissociation limit, and these states are crossed by singlet states which correlates to the IO_2+O^- dissociation limit. The resulting IO_2 is unstable to dissociation, leading to I and O_2 (35). Alternatively, IO_3^- can photodetach an electron at wavelengths shorter than 263 nm to produce neutral IO_3, which is unstable, dissociating into I and O_2. The photon energy threshold required to

photolyze the iodate ion, ~ 260 nm (Fig. S1), corresponds to a wavelength range that has a rapidly increasing actinic flux intensity in the middle stratosphere (Fig. S2). Based on these calculations and the experimental absorption spectrum of iodate (33, 34), we compute the vertical profile of the iodate photolysis rate, which shows a very large increase in its normalized photolytic efficiency from the lower to the upper stratosphere (Fig. S3). These results indicate that despite the bulk of iodine injected to the stratosphere being particulate iodate, it can undergo increasing photo-fragmentation and thereby release iodine back to the gas phase, as air ascends into the tropical middle to upper stratosphere, following the general stratospheric circulation. It is therefore very likely that most, if not all, of the particulate iodate transported to the stratosphere will eventually be photo-activated back to the gas phase during stratospheric transport from the tropics to the Antarctic region.

We performed a set of different Specified-Dynamics WACCM simulations (Methods and Table 1) to assess the iodine effect on Antarctic stratospheric ozone loss, and to identify the spatial, vertical, and temporal extent of these impacts. Based on the experimental evidence and our theoretical analysis of iodate photo-fragmentation, our base simulation (iodine run) considers all iodine to be in gas phase. The ozone differences are computed against a benchmark simulation without iodine. An additional sensitivity was performed without emissions of biogenic bromine VSLS, in order to compare the relative contribution of iodine to total ozone loss with that of brominated VSLS. Hereafter, we focus on the results from the base simulation, which we consider the most likely scenario.

Antarctic stratospheric ozone depletion by iodine

We estimate that iodine chemistry accounts for a mean Antarctic spring (September and October) ozone loss of ~3% of the integrated stratospheric column, averaged during the 1980-2015 simulation period in the 90º-70ºS region (Fig. 1). Iodine causes relatively larger ozone loss at the lower part of the stratospheric ozone hole (11% in the 13-17 km range averaged for spring during the simulation period, and up to 18% at 14km (approx. 140hPa) in spring 1993 (Fig. 2). Overall, the effect of iodine on Antarctic stratospheric ozone is mainly located in the altitude range spanning from the tropopause to about 17 km (Fig. 1 panel c).

The inclusion of iodine leads to a slight improvement in the comparison of modeled total column ozone (TCO) in Antarctica with SBUV-MOD (Solar Backscatter Ultraviolet instrument – Merged Ozone Dataset) satellite observations during the 1980-2015 period (Fig. 3). Note that while there is a good agreement between our model run without iodine and previous state-of-the-art WACCM model simulations (29), our model run with iodine helps to close the gap between previous model simulations and satellite observations (Fig. 3). The simulation including iodine also results in a better agreement with ozonesonde climatologies from Antarctic stations (36) (Fig. S4), mainly between 200 and 80 hPa.

The evolution of iodine-driven ozone loss over Antarctica between 1980 and 2015 shows a pronounced seasonal cycle that oscillates from the sunlit months to the winter, with peak ozone losses in the lowermost stratosphere (Fig. 2). The simulations also show that the highest iodine influence on ozone loss occurred at the beginning of the 1990's, after the eruption of Mount Pinatubo on June 15, 1991 (Fig. 2a). This was associated with the enhanced injection of sulfate aerosol particles to the stratosphere from the volcanic eruption, about two orders of magnitude higher than background levels (37), and the subsequent increase in heterogeneous recycling of not only iodine, but also bromine and chlorine, over those substrates (reactions in Table S4). The results indicate that the iodine impact on ozone during the 1980-2015 period peaked in the post-Pinatubo years (Fig. S5)), implying the sensitivity of spring iodine ozone loss to iodine recycling on stratospheric aerosols and inter-halogen cycling with bromine and chlorine (see next section).

We now explore the iodine influence on the spatio-temporal development of the Antarctic ozone hole. In absolute terms, the effect of iodine on Antarctic stratospheric ozone loss in the 13-17 kms altitude range is approximately constant during most of the year, destroying ~40 ppbv (~4%) (Fig. 4a and Fig. S6), although it is during spring when the relative effect is higher (up to 50 ppbv or 10%). Iodine chemistry also influences the initial formation and closure stages of the ozone hole (Fig. 4b). The results show that considering iodine advances the beginning by about 5 days and delays the closure of the ozone hole (3-5 days) (Fig. 4b). Note that the iodine simulation has a lower stratospheric ozone baseline and therefore the total ozone column drops below the 220 DU threshold that defines the ozone hole region earlier in the season. However, the delay in the closure is due to the ongoing ozone loss by photolysis of OIO, J(OIO), which is the dominant pathway for iodine-driven ozone loss during summer and fall (Fig. S7). The ozone loss rates for the three halogen families increase at the same time during spring, however, from October to December the only ozone loss channel that maintains its spring efficiency is that of J(OIO) (Fig. S7). Iodine also affects the size of the ozone hole area expanding its geographical extension by ~11% or 1.2 million km^2 (Fig. 5), mostly at the beginning of spring (Fig. 4). In addition to the timing and area, the inclusion of iodine also alters the ozone hole mass deficit (defined as the total amount of mass that is deficit relative to the amount of mass present for a value of 220 Dobson Units (DU) (https://ozonewatch.gsfc.nasa.gov), being ~20% lower than in the simulation without iodine.

The relative importance of iodine compared to bromine and chlorine

The contribution of iodine chemical cycles (IO_x^{loss} cycles, see definition of loss cycles in Methods) to ozone loss rates peaks in September (2.5×10^4 molecules cm^{-3} s^{-1}) and then decreases to an approximately constant value (~1×10^4 molecules cm^{-3} s^{-1}) during the rest of the sunlit months (Fig. 6). The inter-halogen crossed $ClO_xBrO_x^{loss}$ cycles follow a similar seasonality although their spring rate (up to 1×10^6 molecules cm^{-3} s^{-1}) is almost two orders of magnitude higher than in summer/autumn (~8×10^3 molecules cm^{-3} s^{-1}). This is related to the seasonality of the heterogeneous reactivation of chlorine and bromine radicals on polar stratospheric clouds (PSCs), which drive and dominate most of the catalytic ozone destruction within the ozone hole (8). However, the IO_x^{loss} seasonal cycle is less pronounced than that of chlorine, indicating that iodine-driven ozone loss is not as sensitive to heterogeneous reactivation since iodine´s gas-phase photochemical cycling is faster than those of bromine and chlorine (17, 38). IO_x^{loss} is dominated by J(OIO), which, together with the IO_HO_2 and the IO_BrO channels, drive the baseline ozone destruction by iodine in the stratosphere. However, during spring, due to the reactivation of chlorine, the IO_ClO cycle increases strongly and even slightly exceeds the J(OIO) channel, depleting ozone by cross reactions with chlorine (Fig. S6b, S6c and Fig. S7). During summer, when heterogeneous recycling does not occur, the channel IO_BrO is more important than the IO_ClO and equals the channel IO_HO_2, with all being less efficient than the loss by OIO photolysis.

Chlorine activation from unreactive (e.g. $ClONO_2$, HCl) to more photochemically reactive (e.g. Cl_2, HOCl) species occurs on the surface of PSCs, during the Antarctic winter and spring (6, 39). Chlorine activation requires the presence of PSCs, and therefore its major contribution to ozone depletion is mainly restricted to springtime. However, the photo-activation of iodine chemistry occurs mainly in the gas phase, therefore, this lack of dependence upon the presence of PSCs results in efficient iodine-driven ozone loss during the entire sunlit period (Fig. 6) and both inside and outside the polar vortex (Fig. S7). Our simulations show that IO_x^{loss} represents ~7% of the halogen-driven ozone destruction in spring, and ~65% in summer, at 13-17 km in the 90ºS-60ºS region (Figure 6a and 6b). Therefore, while iodine-mediated ozone destruction can be significant, although comparatively much smaller than that of ClO_xBrO_x cycles in spring, IO_x^{loss} dominates the halogen-driven ozone destruction chemistry in the Antarctic lower stratosphere during summer (Fig. 6). This summertime destruction of ozone is driven both by J(OIO) and IO+HO_2 (which is

thought to be largely natural) and by IO+BrO (which is dominated by anthropogenic contributions), see Figure S7.

In absolute terms, the most important ozone depleting families are chlorine and bromine, although the abundance of each family is also very different (0.7, 13 and 1335 pptv for I_y, Br_y and Cl_y respectively in this model - see total inorganic bromine, chlorine and iodine definitions in Materials and Methods -, at the 16 km altitude in the 90ºS-60ºS region). Thus, the ozone depletion efficacy of each family on a per atom basis can be estimated by normalizing the ozone loss rates of each family by their corresponding inorganic halogen abundance (i.e., I_y, Br_y and Cl_y concentration). Fig. S8 shows that the family with highest ozone depletion efficacy is iodine, followed by bromine and with a much smaller value for chlorine.

The ozone loss caused by the currently estimated 5.0±2.1 pptv of biogenic brominated VSLS that enter the stratosphere has been a subject of research in the last two decades (13–16, 40). Here we compare Antarctic lower stratospheric (90ºS-70ºS at 13-17 km altitude) ozone loss driven by oceanic iodine emissions with that of biogenic bromine (Fig. S6). During summer and fall, 0.77 pptv of iodine leads to a baseline ozone loss of ~ 40 ppbv, while 5 ppt of biogenic bromine accounts for a baseline loss of ~45 ppbv. In spring, the ozone loss increases to 50 ppbv and 96 ppbv O_3 for iodine and biogenic bromine, respectively (Fig. S6). We estimate that the ozone loss caused by 0.77 pptv of iodine in the Antarctic lower stratosphere is equivalent to 2.8 pptv and 4.42 pptv of biogenic brominated VSLS in spring and the rest of the sunlit period, respectively.

The larger stratospheric ozone depletion efficacy of iodine compared to equivalent amounts of bromine, highlights the potential importance that iodine chemistry can have under different halogen loading scenarios. In the future, the influence of anthropogenic long-lived ozone depleting substances containing chlorine and bromine will decrease due to the Montreal Protocol, which in turn will increase the relative contribution of chlorinated and brominated VSLS emitted from the oceans (13, 41). Ocean iodine emissions have tripled since 1950 (42–44), and it has been proposed that oceanic emissions of inorganic iodine may increase by ~20% following RCP 8.5 over the 2000-2100 period (30). Consequently, the future relative contribution of iodine to the stratospheric ozone loss may likely be higher than at present, with potential implications in delaying the future closing of the ozone hole, which warrant further investigation.

In summary, while we acknowledge existing uncertainties in iodine gas-to-particle partitioning and heterogeneous recycling of iodine reservoirs, as well as the need for observations of iodine in the Antarctic stratosphere, our results imply that the iodine contribution to chemical ozone destruction in the Antarctic ozone hole can potentially be significant, particularly in the lowermost stratosphere. Iodine-atom catalysed ozone depletion has been neglected in the research of the Antarctic ozone hole since its discovery, due to the negligible amounts of iodine previously thought to enter the stratosphere (23). However, based on the recent quantification of stratospheric iodine injection (24, 25), our results suggest that iodine injection and chemistry need to be considered in models, along with chlorine and bromine, for fully accurate assessments of halogen-mediated impacts on the background ozone abundances and ozone depletion in the Antarctic stratosphere.

Materials and Methods

WACCM REFC1SD configuration

In this work we have employed the Community Earth System Model, version 1 (CESM1), with the Whole Atmosphere Community Climate Model, version 4 (WACCM4) (26) as the atmospheric component. WACCM4 is a fully coupled state-of-the-art interactive chemistry climate model (45). The model setup is based on the specified dynamics version of WACCM4 (SD-WACCM), including reanalysis for temperature, zonal and meridional winds, as well as surface pressure fields from the Modern Era Retrospective Analysis for Research and Applications (MERRA2) (28, 46, 47). The standard WACCM chemical scheme includes the O_x, NO_x, HO_x, ClO_x, and BrO_x chemical families, along with gas phase and heterogeneous reactions on liquid binary and ternary sulfate polar stratospheric cloud particles, as well as solid nitric acid trihydrate and water ice polar stratospheric particles (48). The model (29) also incorporates an updated halogen chemistry scheme for halogens (chlorine, bromine, and iodine), as described in the following section.

Very Short-Lived halogen implementation in WACCM

The benchmark WACCM4 troposphere-stratosphere-mesosphere-and-lower-thermosphere (TSMLT) chemical scheme was updated to include previous developments of very short-lived (VSL) tropospheric halogen chemistry already implemented in the CAM-Chem4 version of CESM1 (31, 32, 49). This includes the off-line emission of oceanic VSL chloro-, bromo-, and iodo-carbons, the on-line computation of the sea-salt aerosol (SSA) dehalogenation source due to the effective uptake of chloride and bromide from SSA, as well as the heterogeneous reactivation of inorganic halogen reservoirs on top of ice-crystals in the upper troposphere (13, 31, 50). For the particular case of iodine chemistry, additional sources of inorganic iodine (in the form of HOI and I_2) due to the ozone-driven oxidation of aqueous iodide occurring at the ocean surface were also considered (30, 51–53). Note that this additional oceanic source of inorganic iodine is computed on-line based on modeled surface ozone and accounts for up to 60% of the current total inorganic iodine within the tropical tropopause layer (25), representing a significant contribution to the modeled stratospheric iodine injection. Regarding the chemical scheme, subsequent CAM-Chem updates mapping the heterogeneous recycling of $IONO_2$ and HOI on upper tropospheric ice-crystals have also been included based in Saiz-Lopez et al., (2015) (24), which in turn considers the formation and photolysis of higher order iodine oxides (J-I_xO_y scheme, see Saiz-Lopez et al., 2014 (32)). Table S2 in the Supporting Information material from Saiz-Lopez et al., (2015) (24) compiles the individual inorganic iodine species that undergo washout and ice-uptake within the model, as well as the specific parameterization and/or approximation used in each case.

Within the stratosphere, we mapped the standard scheme of heterogeneous recycling reactions for bromine and chlorine species (29, 54) to apply also for iodine (see Table S4). Even when the heterogeneous recycling of iodine species is expected to be faster than for the other halogens, and due to the scarcity of laboratory measurements (38), we mapped all reactive-uptake coefficients (gammas) to those values from the equivalent brominated reactions (reactions in blue in Table S4). However, and given the much larger photolytic efficiency of iodine species, the heterogeneous reactivation of iodine reservoirs represents only a minor contribution and gas-phase photochemistry dominates iodine reactivation (17). In this regard, note that both CAM-Chem and WACCM include a logical condition based on the location of the local tropopause to allow for the stratospheric heterogeneous reactivation of halogen reservoirs on different types of aerosol surfaces, including Sulfate (SULF), Nitric Acid Trihydrate (NAT) and Polar Stratospheric Clouds (PSCs) substrates, whose surface area density (SAD) and effective radius are computed on-line (29). However, as WACCM includes a detailed treatment of stratosphere-to-troposphere exchange (STE), these processes can result also in significant changes within the upper troposphere and lower stratosphere (UTLS) composition.

Finally, within the “iodine run” scheme we assume that all the particulate iodine injected to the stratosphere is completely photolyzed back to gas-phase iodine due to the rapid enhancement of UV radiation in the upper stratosphere (see Fig. S3). This assumption is justified based on the particulate iodine speciation that shows that the dominant fraction of iodine in UTLS is iodate (25), as well as on the experimental and theoretical determination of the iodate absorption spectra, that shows a maximum photodissociation efficiency within the 200-285 nm range (33, 34). The normalized enhancement in the photodisociation efficiency of particulate iodine (J-iodine, assuming all iodine in the aerosol in iodate) increases up to 8 orders of magnitude between 10 and 40 km, highlighting the rapid re-conversion of particulate iodate into gas-phase I_y.

Model runs

All model runs have been performed in specified dynamics mode (REFC1-SD) (55), with dynamics specified from reanalysis (56) between 1980 and 2015. Three different configurations have been run as follows (Table 1): i) the “iodine” run, from 1980 to 2015, includes updated iodine chemistry and emissions of both iodine (organic: CH_2I_2, CH_2IBr, CH_2ICl, CH_3I and inorganic: I_2, and HOI) and biogenic bromine ($CHBr_3$, CH_2Br_2, CH_2BrCl, $CHBr_2Cl$ and $CHBrCl_2$) VSLs species; ii) the “no Br VSLs” run in which the emissions of biogenic bromine VSLs from the oceans are disabled, to account for the ozone depletion caused by these bromine species; and iii) the “no iodine” run, in which all iodine sources, both organic and inorganic, are disabled. Therefore, the net iodine influence on the ozone hole formation can be addressed by comparing the “iodine” vs. “no iodine” runs, while the relative comparison between biogenic iodine and bromine to Antarctic stratospheric ozone depletion can be estimated from “iodine” vs “no Br VSLs” cases. This is the WACCM state-of-the-art simulation employed in previous works on polar stratospheric ozone (29, 57). WACCM was configured with a horizontal resolution of 1.9° latitude by 2.5° longitude and 88 levels, from the surface to ~130 km, as in previous studies (29)

Total inorganic bromine, chlorine and iodine definitions:
$Br_y = Br+BrO+HOBr+BrONO_2+HBr+BrCl+2Br_2+BrNO_2+IBr$
$Cl_y = Cl+ClO+2Cl_2+2Cl_2O_2+OClO+HOCl+ClONO_2+HCl+BrCl+ClNO_2+ICl$
$I_y = I+2I_2+IO+OIO+HI+HOI+INO+INO_2+IONO_2+IBr+ICl+2I_2O_2+2I_2O_3+2I_2O_4$

Ozone loss rates definitions for the different families, including halogens (ClO_x, BrO_x, IO_x and the crossed inter-halogen cycles ClO_xBrO_x), O_x ($O+O_3$), HO_x ($H+OH+HO_2$)) and NO_x ($NO+NO_2$):

$ClOx^{loss} = 2 \times ClO\_O + 2 \times J(Cl_2O_2) + 2 \times ClO\_ClOa + 2 \times ClO\_ClOb + ClO\_HO_2$

$ClO + O \rightarrow Cl + O_2$	ClO_O
$Cl_2O_2 + hv \rightarrow 2\times Cl$	$J(Cl_2O_2)$
$ClO + ClO \rightarrow 2\times Cl + O_2$	ClO_ClOa
$ClO + ClO \rightarrow Cl_2 + O_2$	ClO_ClOb
$ClO + HO_2 \rightarrow O_2 + HOCl$	ClO_HO_2

$BrOx^{loss} = 2 \times BrO\_BrO + 2 \times BrO\_O + BrO\_HO_2$

$BrO + BrO \rightarrow 2\times Br + O_2$	BrO_BrO
$BrO + O \rightarrow Br + O_2$	BrO_O
$BrO + HO_2 \rightarrow HOBr + O_2$	BrO_HO_2

$ClOxBrOx^{loss} = 2 \times BrO\_ClOb + 2 \times BrO\_ClOc$

$BrO + ClO \rightarrow Br + Cl + O_2$	BrO_ClOb
$BrO + ClO \rightarrow BrCl + O_2$	BrO_ClOc

$IOx^{loss} = 2 \times IO\_O + 2 \times J(OIO) + IO\_HO_2 + 2 \times IO\_BrOa + 2 \times IO\_ClOb + 2 \times IO\_ClOc$

$IO + O \rightarrow I + O_2$	IO_O

$OIO + hv \rightarrow I + O_2$	J(OIO)
$IO + HO_2 \rightarrow HOI + O_2$	IO_HO_2
$IO + BrO \rightarrow Br + I + O_2$	IO_BrOa
$IO + ClO \rightarrow I + Cl + O_2$	IO_ClOb
$IO + ClO \rightarrow ICl + O_2$	IO_ClOc

Ox^{loss} = 2 × O_O_3 + O(^{1}D)_H_2O

$O + O_3 \rightarrow 2O_2$	O_O_3
$O(^1D) + H_2O \rightarrow 2OH$	O(^{1}D)_H_2O

HOx^{loss} = HO_2_O + HO_2_O_3 + OH_O + OH_O_3 + H_O_3

$HO_2 + O \rightarrow OH + O_2$	HO_2_O
$HO_2 + O_3 \rightarrow OH + 2*O_2$	HO_2_O_3
$OH + O \rightarrow H + O_2$	OH_O
$OH + O_3 \rightarrow HO_2 + O_2$	OH_O_3
$H + O_3 \rightarrow OH + O_2$	H_O_3

NOx^{loss} = 2 × NO_2_O + 2 × J(NO_3)

NO_2 + O -> NO + O_2	NO_2_O
NO_3 + hv -> NO + O_2	J(NO_3)

Acknowledgments

This study received funding from the European Research Council Executive Agency under the European Union's Horizon 2020 Research and Innovation Programme (Project ERC-2016- COG 726349 CLIMAHAL). DK is partly supported by NASA grant (80NSSC19K0952). SS is partly supported by NSF-AGS grant 1906719. Computing resources, support, and data storage were provided by the Climate Simulation Laboratory at NCAR's Computational and Information Systems Laboratory (CISL), sponsored by the NSF. R.P.F would like to thanks CONICET, UNCUYO (SIIP M032/3853) and FONCYT (PICT 2019-02187) for financial support.

References

1. M. J. Molina, F. S. Rowland, Stratospheric sink for chlorofluoromethanes: chlorine atom-catalysed destruction of ozone. *Nature* **249**, 810–812 (1974).

2. J. C. Farman, B. G. Gardiner, J. D. Shanklin, Large losses of total ozone in Antarctica reveal seasonal ClOx/NOx interaction. *Nature* **315**, 207–210 (1985).

3. R. S. Stolarski, *et al.*, Nimbus 7 satellite measurements of the springtime Antarctic ozone decrease. *Nature* **322**, 808–811 (1986).

4. R. L. de Zafra, *et al.*, High concentrations of chlorine monoxide at low altitudes in the Antarctic spring stratosphere: diurnal variation. *Nature* **328**, 408–411 (1987).

5. C. B. Farmer, G. C. Toon, P. W. Schaper, J.-F. Blavier, L. L. Lowes, Stratospheric trace gases in the spring 1986 Antarctic atmosphere. *Nature* **329**, 126–130 (1987).

6. S. Solomon, G. H. Mount, R. W. Sanders, A. L. Schmeltekopf, Visible spectroscopy at McMurdo Station, Antarctica: 2. Observations of OClO. *J. Geophys. Res. Atmos.* **92**, 8329–8338 (1987).

7. J. G. Anderson, D. W. Toohey, W. H. Brune, Free Radicals Within the Antarctic Vortex:

The Role of CFCs in Antarctic Ozone Loss. *Science (80-.).* **251**, 39 LP – 46 (1991).

8. S. Solomon, Stratospheric ozone depletion: A review of concepts and history. *Rev. Geophys.* **37**, 275–316 (1999).

9. M. B. McElroy, R. J. Salawitch, S. C. Wofsy, J. A. Logan, Reductions of Antarctic ozone due to synergistic interactions of chlorine and bromine. *Nature* **321**, 759–762 (1986).

10. S. A. Montzka, J. H. Butler, B. D. Hall, D. J. Mondeel, J. W. Elkins, A decline in tropospheric organic bromine. *Geophys. Res. Lett.* **30** (2003).

11. B.-M. Sinnhuber, N. Sheode, M. Sinnhuber, M. P. Chipperfield, W. Feng, The contribution of anthropogenic bromine emissions to past stratospheric ozone trends: a modelling study. *Atmos. Chem. Phys.* **9**, 2863–2871 (2009).

12. M. Dorf, *et al.*, Long-term observations of stratospheric bromine reveal slow down in growth. *Geophys. Res. Lett.* **33** (2006).

13. R. P. Fernandez, D. E. Kinnison, J. F. Lamarque, S. Tilmes, A. Saiz-Lopez, Impact of biogenic very short-lived bromine on the Antarctic ozone hole during the 21st century. *Atmos. Chem. Phys.* **17**, 1673–1688 (2017).

14. World Meteorological Organization (WMO), Scientific Assessment of Ozone Depletion: 2018 Global Ozone Research and Monitoring Project Report 58 (2018).

15. P. A. Wales, *et al.*, Stratospheric Injection of Brominated Very Short-Lived Substances: Aircraft Observations in the Western Pacific and Representation in Global Models. *J. Geophys. Res. Atmos.* **123**, 5690–5719 (2018).

16. R. J. Salawitch, *et al.*, Sensitivity of ozone to bromine in the lower stratosphere. *Geophys. Res. Lett.* **32** (2005).

17. S. Solomon, R. R. Garcia, A. R. Ravishankara, On the role of iodine in ozone depletion. *J. Geophys. Res. Atmos.* **99**, 20491–20499 (1994).

18. A. Butz, *et al.*, Constraints on inorganic gaseous iodine in the tropical upper troposphere and stratosphere inferred from balloon-borne solar occultation observations. *Atmos. Chem. Phys.* **9**, 7229–7242 (2009).

19. G. Berthet, J.-B. Renard, M. Chartier, M. Pirre, C. Robert, Analysis of OBrO, IO, and OIO absorption signature in UV-visible spectra measured at night and at sunrise by stratospheric balloon-borne instruments. *J. Geophys. Res. Atmos.* **108** (2003).

20. H. Bösch, *et al.*, Upper limits of stratospheric IO and OIO inferred from center-to-limb-darkening-corrected balloon-borne solar occultation visible spectra: Implications for total gaseous iodine and stratospheric ozone. *J. Geophys. Res. Atmos.* **108** (2003).

21. I. Pundt, J.-P. Pommereau, C. Phillips, E. Lateltin, Upper Limit of Iodine Oxide in the Lower Stratosphere. *J. Atmos. Chem.* **30**, 173–185 (1998).

22. P. O. Wennberg, J. W. Brault, T. F. Hanisco, R. J. Salawitch, G. H. Mount, The atmospheric column abundance of IO: Implications for stratospheric ozone. *J. Geophys. Res. Atmos.* **102**, 8887–8898 (1997).

23. World Meteorological Organization (WMO), *Scientific Assessment of Ozone Depletion: 2014* (2014).

24. A. Saiz-Lopez, *et al.*, Injection of iodine to the stratosphere. *Geophys. Res. Lett.* **42** (2015).

25. T. K. Koenig, *et al.*, Quantitative detection of iodine in the stratosphere. *Proc. Natl. Acad. Sci. U. S. A.* **117** (2020).

26. R. B. Neale, *et al.*, The Mean Climate of the Community Atmosphere Model (CAM4) in Forced SST and Fully Coupled Experiments. *J. Clim.* **26**, 5150–5168 (2013).

27. D. R. Marsh, *et al.*, Climate Change from 1850 to 2005 Simulated in CESM1(WACCM). *J. Clim.* **26**, 7372–7391 (2013).

28. R. R. Garcia, A. K. Smith, D. E. Kinnison, Á. de la Cámara, D. J. Murphy, Modification of the Gravity Wave Parameterization in the Whole Atmosphere Community Climate Model: Motivation and Results. *J. Atmos. Sci.* **74**, 275–291 (2017).

29. S. Solomon, D. Kinnison, J. Bandoro, R. Garcia, Simulation of polar ozone depletion: An update. *J. Geophys. Res. Atmos.* **120**, 7958–7974 (2015).

30. F. Iglesias-Suarez, *et al.*, Natural halogens buffer tropospheric ozone in a changing climate. *Nat. Clim. Chang.* (2020) https:/doi.org/10.1038/s41558-019-0675-6.

31. R. P. Fernandez, R. J. Salawitch, D. E. Kinnison, J.-F. Lamarque, A. Saiz-Lopez, Bromine partitioning in the tropical tropopause layer: implications for stratospheric injection. *Atmos. Chem. Phys.* **14**, 13391–13410 (2014).

32. A. Saiz-Lopez, *et al.*, Iodine chemistry in the troposphere and its effect on ozone. *Atmos. Chem. Phys.* **14**, 13119–13143 (2014).

33. Ó. Gálvez, M. T. Baeza-Romero, M. Sanz, A. Saiz-Lopez, Photolysis of frozen iodate salts as a source of active iodine in the polar environment. *Atmos. Chem. Phys.* **16**, 12703–12713 (2016).

34. K. Kim, *et al.*, Nitrite-Induced Activation of Iodate into Molecular Iodine in Frozen Solution. *Environ. Sci. Technol.* **53**, 4892–4900 (2019).

35. J. C. Gómez Martín, S. H. Ashworth, A. S. Mahajan, J. M. C. Plane, Photochemistry of OIO: Laboratory study and atmospheric implications. *Geophys. Res. Lett.* **36** (2009).

36. S. Tilmes, *et al.*, Technical Note: Ozonesonde climatology between 1995 and 2011: description, evaluation and applications. *Atmos. Chem. Phys.* **12**, 7475–7497 (2012).

37. M. J. Mills, *et al.*, Global volcanic aerosol properties derived from emissions, 1990–2014, using CESM1(WACCM). *J. Geophys. Res. Atmos.* **121**, 2332–2348 (2016).

38. A. Saiz-Lopez, *et al.*, Atmospheric Chemistry of Iodine. *Chem. Rev.* **112**, 1773–1804 (2012).

39. P. J. Crutzen, F. Arnold, Nitric acid cloud formation in the cold Antarctic stratosphere: a major cause for the springtime 'ozone hole.' *Nature* **324**, 651–655 (1986).

40. L. D. Oman, *et al.*, The effect of representing bromine from VSLS on the simulation and evolution of Antarctic ozone. *Geophys. Res. Lett.* **43**, 9869–9876 (2016).

41. R. Hossaini, *et al.*, Efficiency of short-lived halogens at influencing climate through depletion of stratospheric ozone. *Nat. Geosci.* **8**, 186–190 (2015).

42. C. A. Cuevas, *et al.*, Rapid increase in atmospheric iodine levels in the North Atlantic since the mid-20th century. *Nat. Commun.* **9** (2018).

43. M. Legrand, *et al.*, Alpine ice evidence of a three-fold increase in atmospheric iodine deposition since 1950 in Europe due to increasing oceanic emissions. *Proc. Natl. Acad. Sci. U. S. A.* **115** (2018).

44. X. Zhao, X. Hou, W. Zhou, Atmospheric Iodine (127I and 129I) Record in Spruce Tree Rings in the Northeast Qinghai-Tibet Plateau. *Environ. Sci. Technol.* **53**, 8706–8714 (2019).

45. V. Eyring, T. G. Shepherd, D. W. Waugh, Eds., "SPARC CCMVal Report on the Evaluation of Chemistry-Climate Models" (SPARC Office, 2010).

46. R. Gelaro, *et al.*, The Modern-Era Retrospective Analysis for Research and Applications, Version 2 (MERRA-2). *J. Clim.* **30**, 5419–5454 (2017).

47. M. M. Rienecker, *et al.*, MERRA: NASA's Modern-Era Retrospective Analysis for Research and Applications. *J. Clim.* **24**, 3624–3648 (2011).

48. JPL, Chemical Kinetics and Photochemical Data for Use in Atmospheric Studies, vol 15. *JPL Publ. 06-02, Jet Propuls. Lab., Pasadena* (2011).

49. C. Ordóñez, *et al.*, Bromine and iodine chemistry in a global chemistry-climate model: description and evaluation of very short-lived oceanic sources. *Atmos. Chem. Phys.* **12**, 1423–1447 (2012).

50. J. A. Barrera, *et al.*, Seasonal impact of biogenic very short-lived bromocarbons on lowermost stratospheric ozone between 60{\degree}\,N and 60{\degree}\,S during the 21st century. *Atmos. Chem. Phys.* **20**, 8083–8102 (2020).

51. C. Prados-Roman, *et al.*, A negative feedback between anthropogenic ozone pollution and enhanced ocean emissions of iodine. *Atmos. Chem. Phys.* **15** (2015).

52. S. M. MacDonald, *et al.*, A laboratory characterisation of inorganic iodine emissions from the sea surface: dependence on oceanic variables and parameterisation for global modelling. *Atmos. Chem. Phys.* **14**, 5841–5852 (2014).

53. L. J. Carpenter, *et al.*, Atmospheric iodine levels influenced by sea surface emissions of inorganic iodine. *Nat. Geosci.* **6**, 108–111 (2013).

54. D. E. Kinnison, *et al.*, Sensitivity of chemical tracers to meteorological parameters in the MOZART-3 chemical transport model. *J. Geophys. Res. Atmos.* **112** (2007).

55. V. Eyring, *et al.*, Overview of IGAC/SPARC Chemistry-Climate Model Initiative (CCMI) Community Simulations in Support of Upcoming Ozone and Climate Assessments in (2013).

56. S. Tilmes, *et al.*, Representation of the Community Earth System Model (CESM1) CAM4-chem within the Chemistry-Climate Model Initiative (CCMI). *Geosci. Model Dev.* **9**, 1853–1890 (2016).

57. K. A. Stone, S. Solomon, D. E. Kinnison, On the Identification of Ozone Recovery. *Geophys. Res. Lett.* **45**, 5158–5165 (2018).

Figures and Tables

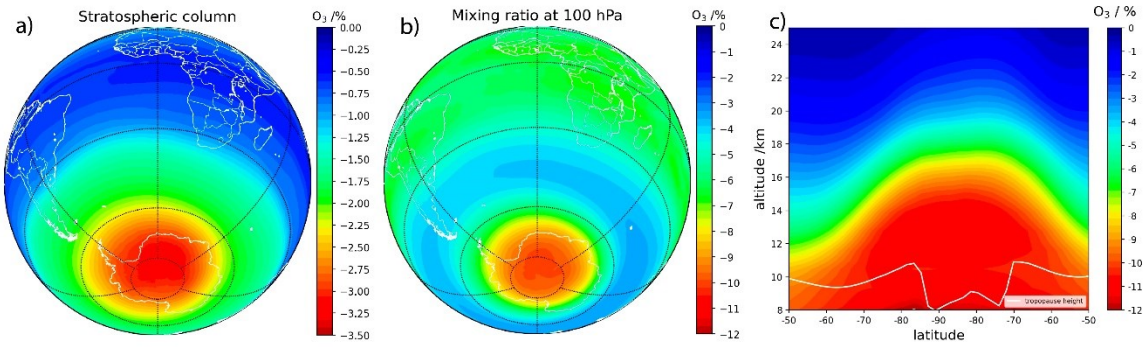

Figure 1. 1980-2015 September-October averaged influence of iodine chemistry on the Antarctic stratospheric ozone depletion: a) percentage impact over the stratospheric vertical column; b) effect at 16 km altitude (~100 hPa); and c) averaged meridional slice at 0º longitude, in which the effect of iodine chemistry can be seen spatially as a function of latitude and altitude. The relative percentage difference has been computed as ((iodine run – no iodine run) / no iodine run) × 100.

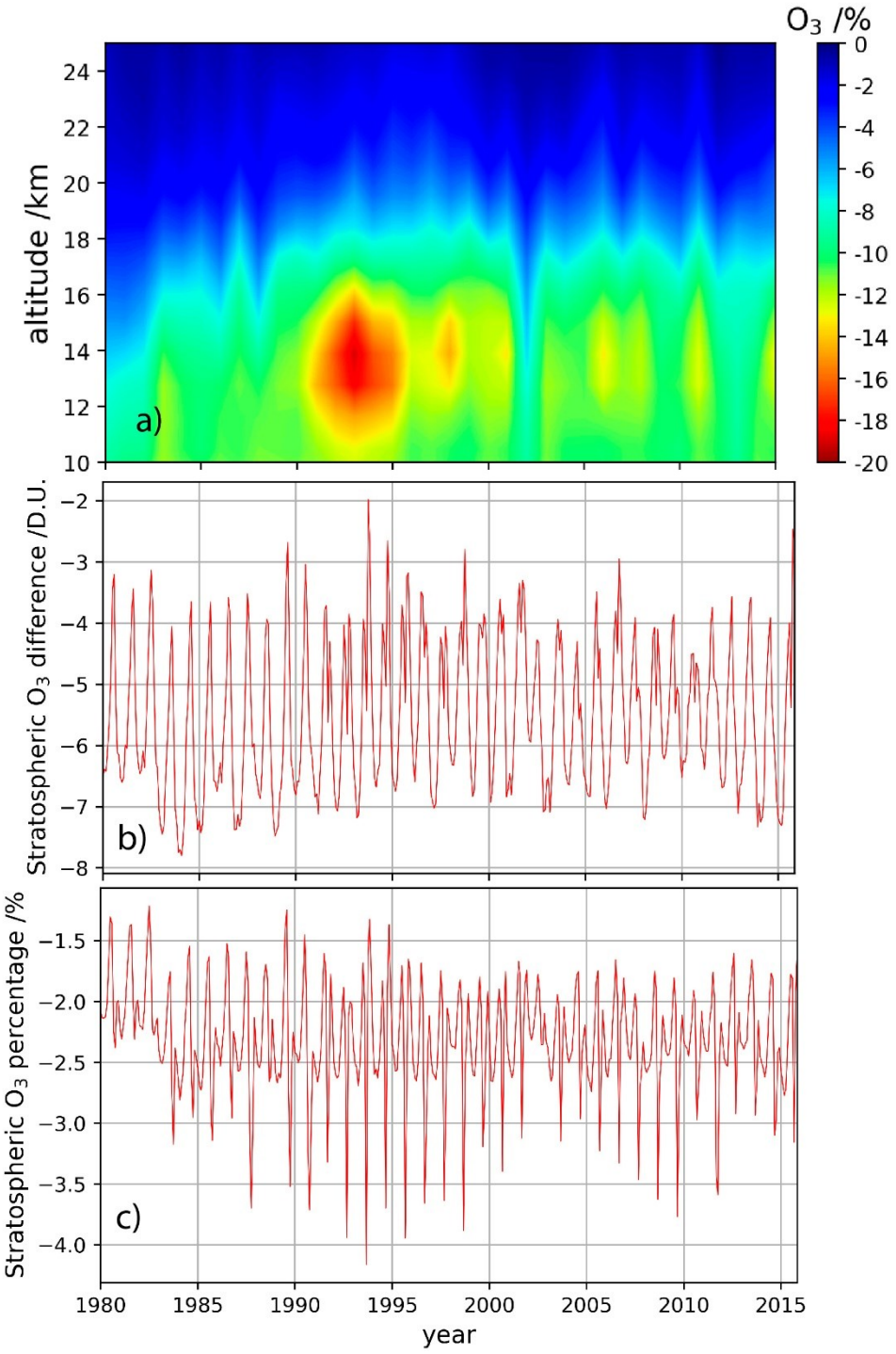

Figure 2. Averaged ozone vertical profile in September and October, in the 90ºS-70ºS region latitude during the 1980-2015 period (a); and monthly averaged iodine effect on the stratospheric ozone vertical column density in the 90ºS-70ºS (b and c).

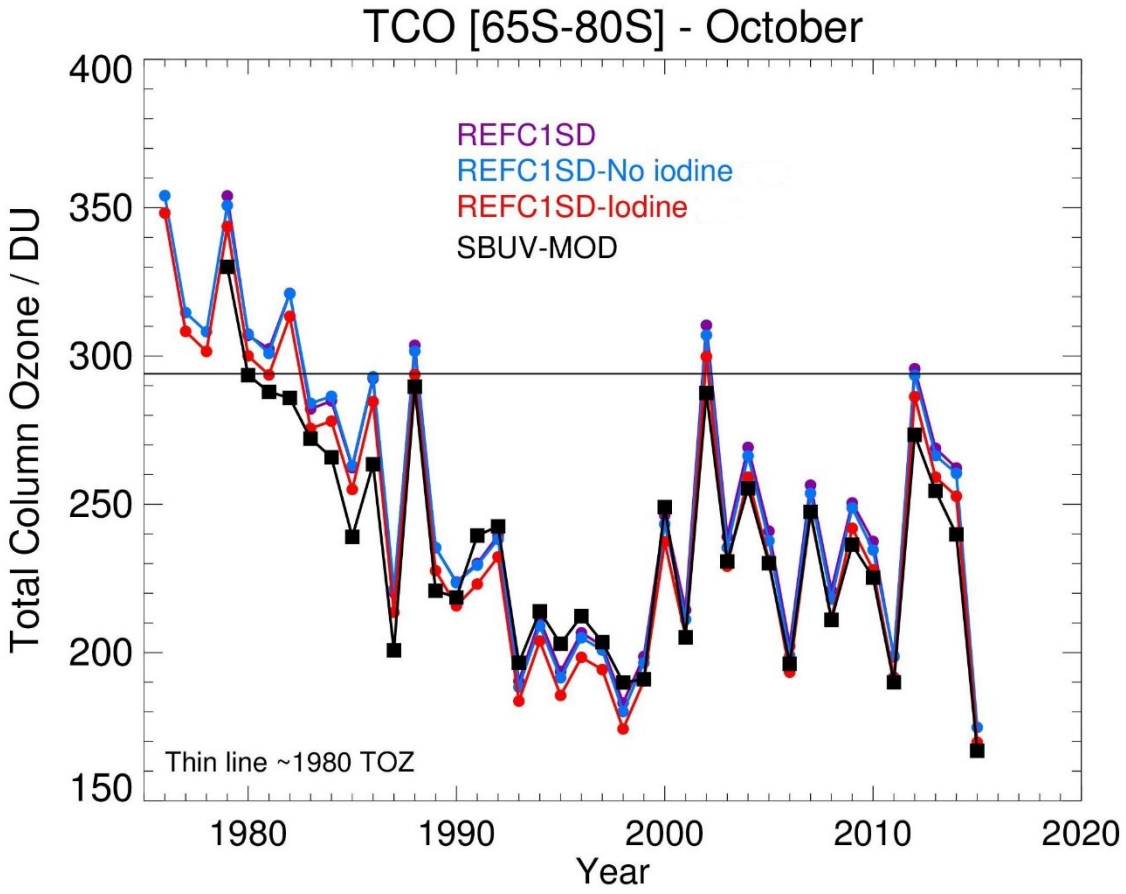

Figure 3. October averaged evolution of the total column ozone (TCO) in Antarctica together with SBUV-MOD satellite data (Solar Backscatter Ultraviolet instrument – Merged Ozone Dataset). REFC1SD is the state-of-the-art WACCM simulation including MAM SAD fields employed in (29). This simulation does not have heterogeneous chemistry on ice, and considers a surface lower boundary conditions (LBC) of 1.2 pptv for $CHBr_3$ and CH_2Br_2 species. The REFC1SD-No iodine run includes the complete VSL Bromine scheme, but no VSL Iodine, and the REFC1SD-Iodine run includes both VSL Bromine and Iodine. Black thin line represents the total ozone column in 1980.

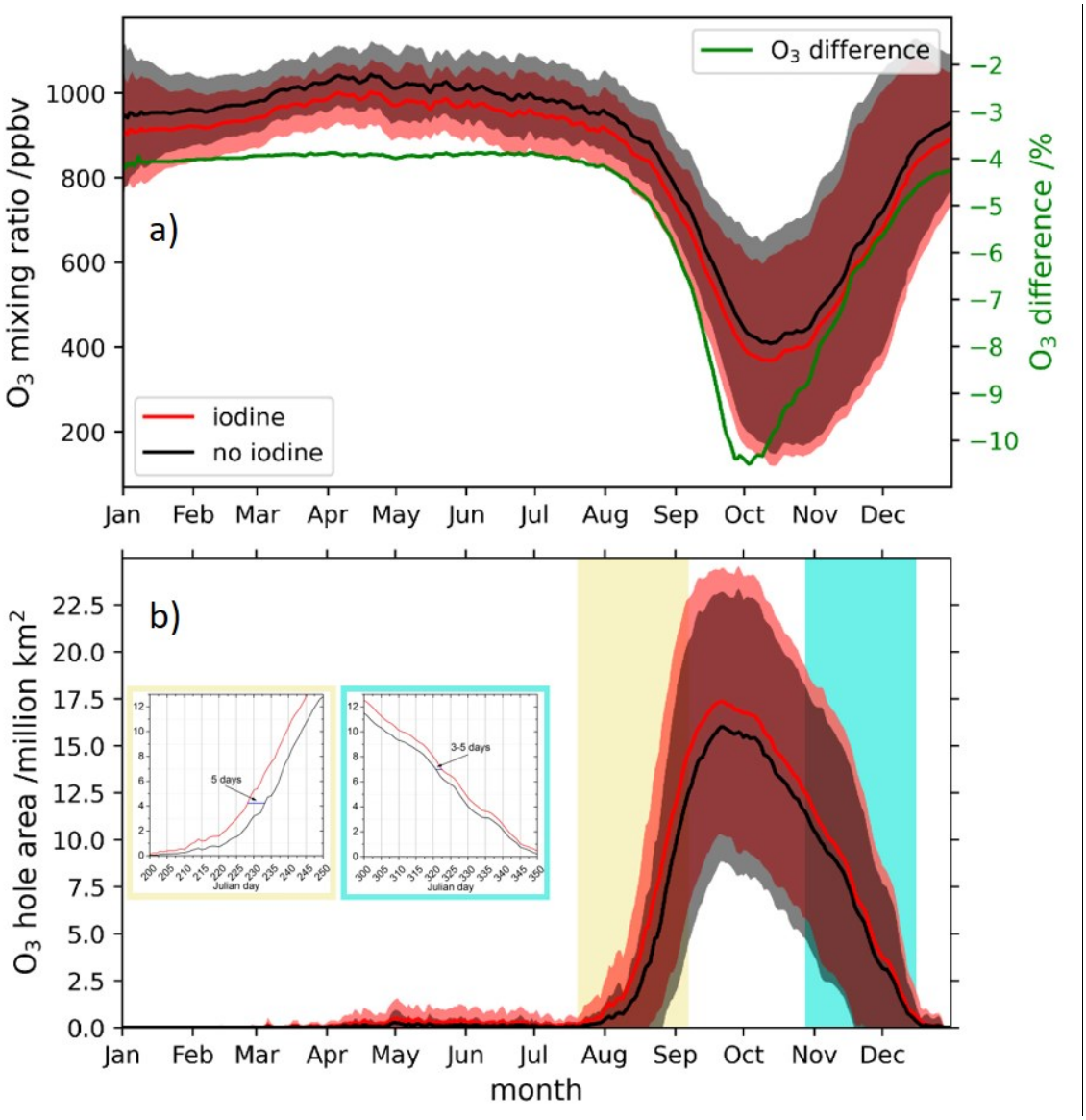

Figure 4. Daily evolution of the ozone hole region during the 1980-2015 period in the region 90ºS-70ºS at 13-17 km altitude for the simulation including the three halogens (red, “iodine”), and the simulation including only bromine and chlorine (black, “no iodine”). Left Y-axis shows the averaged ozone mixing ratio, while green right Y-axis in the a) panel corresponds to the difference (in percentage) between the “iodine” and “no iodine” runs. b) represents the ozone hole area, defined as the region of ozone values below 220 Dobson Units (DU) located south of 40°S (https://ozonewatch.gsfc.nasa.gov).

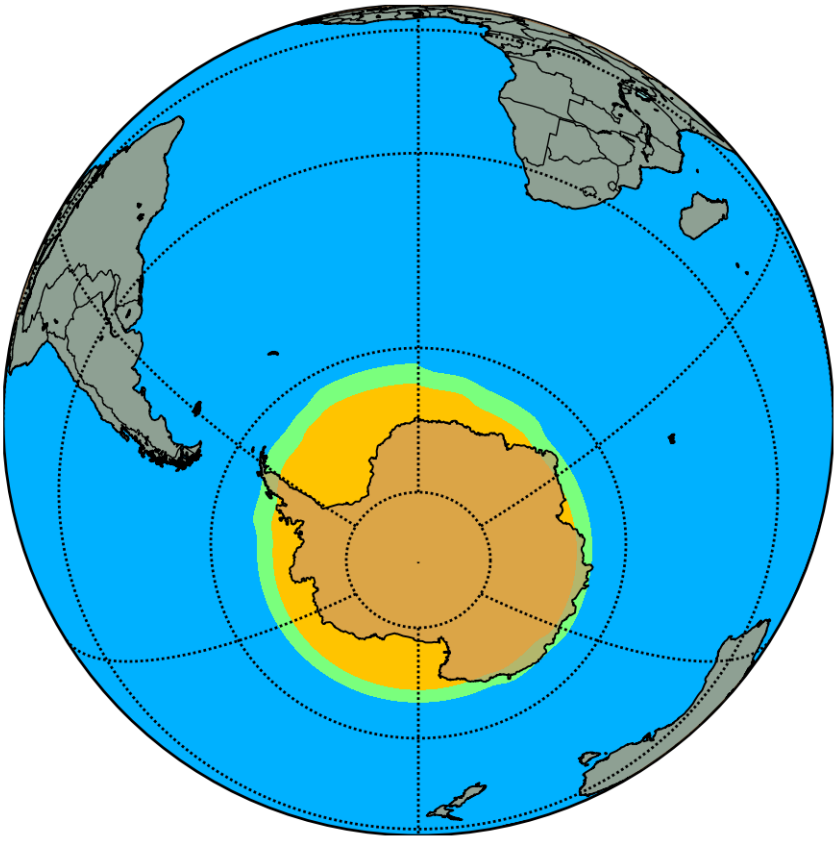

Figure 5. Averaged ozone hole area (TOC < 220 DU) in the Antarctic spring (September and October) during the whole simulation period (1980-2015). The ozone hole area in the simulation without iodine is shown in yellow, while the expansion of the ozone hole area caused by iodine is depicted in green.

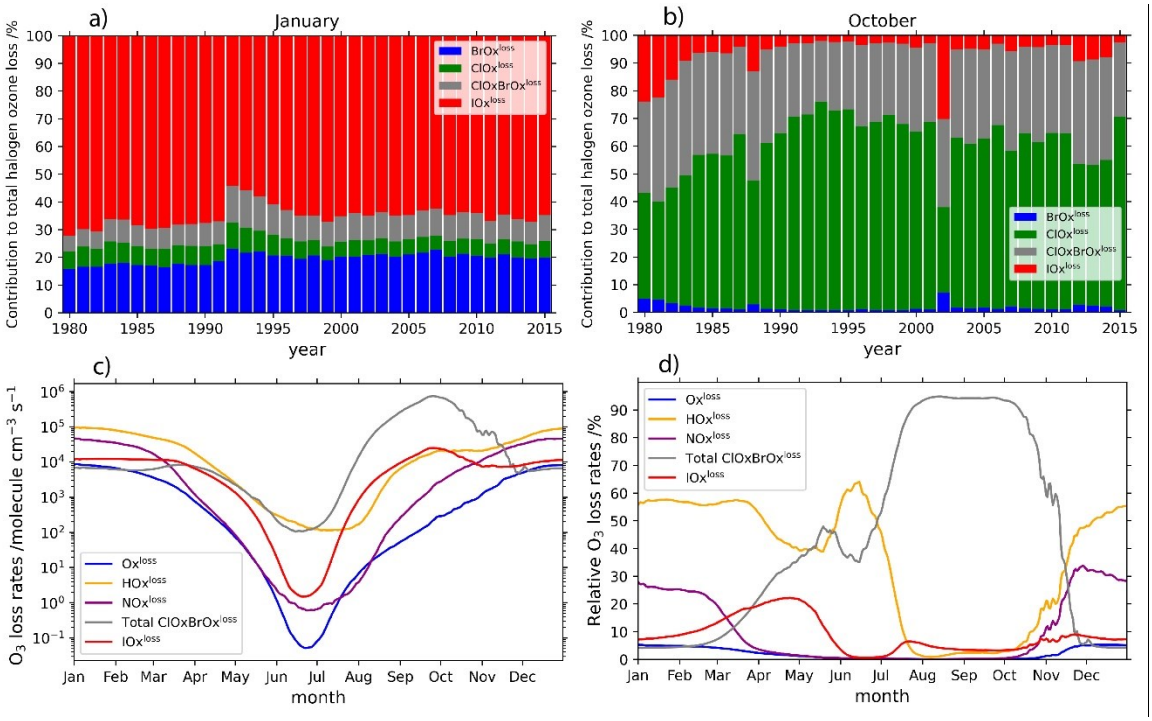

Figure 6. Contribution of iodine chemistry to the evolution of the ozone hole, in terms of ozone loss rates, compared to chlorine and bromine and the rest of families (see definition of ozone loss rates in Materials and Methods). The upper panels (a and b) include the monthly averaged relative contribution of each halogen family with respect to total halogen ozone loss rate during the Antarctic summer (January) and spring (October) for the 1980-2015 period at 13-17 km altitude and 90ºS-70ºS latitude range. The lower panels (c and d) show the daily ozone loss rates averaged during the 1980-2015 period in the same region. In these lower panels the Total $ClO_xBrO_x^{loss}$ term includes all contribution from chlorine and bromine to ozone loss (Total ClO_xBrO_x= ClO_x^{loss} + BrO_x^{loss} + $ClO_xBrO_x^{loss}$ according to ozone loss definitions in Materials and Methods)

Run	Time period	Iodine emissions	Biogenic bromine VSLs emissions
Iodine (base simulation)	1980-2015	Yes	Yes
No Br VSLs	1980-2015	Yes	No
No iodine	1980-2015	No	Yes

Table 1. REFC1SD WACCM4 simulations considered in this study.

PNAS
www.pnas.org

Supplementary Information for

The influence of iodine on the Antarctic stratospheric ozone hole

Carlos A. Cuevas[1,*], Rafael P. Fernandez[2-3], Douglas E. Kinnison[4], Qinyi Li[1], Jean-François Lamarque[5], Tarek Travelsi[6], Joseph S. Francisco[6], Susan Solomon[7], and Alfonso Saiz-Lopez[1,*]

[1]Department of Atmospheric Chemistry and Climate, Institute of Physical Chemistry Rocasolano, CSIC, Madrid, 28006, Spain
[2]Institute for Interdisciplinary Science, National Research Council (ICB-CONICET), Mendoza, 5501, Argentina
[3]School of Natural Sciences, National University of Cuyo (FCEN-UNCuyo), Mendoza, 5501, Argentina
[4]Atmospheric Chemistry Observation and Modeling, National Center for Atmospheric Research, Boulder, CO 80305, USA
[5]Climate and Global Dynamics Laboratory, National Center for Atmospheric Research, Boulder, CO 80305, USA
[6]Department of Chemistry, University of Pennsylvania, Philadelphia, PA 19104, USA
[7]Department of Earth, Atmospheric, and Planetary Sciences, Massachusetts Institute of Technology, Cambridge, MA, 02139, USA

*Corresponding author: Alfonso Saiz-Lopez and Carlos A. Cuevas

Email: a.saiz@csic.es; ccuevas@iqfr.csic.es

This PDF file includes:

Supplementary information test

Theoretical calculations for the destruction of photo-dissociation of iodate

Two plausible mechanisms may lead to the photochemical destruction or the photodissociation of IO_3^-:

Mechanism 1

Table S1 predict the vertical excitation energies for the low-lying electronic states of IO_3^-. Absorption of a photon to these states or to the detachment continuum (hv < 263 nm ADE (1)) lead to the photodetachment. In this case, many products may be produced such as:

$$IO_3^- + hv \rightarrow IO_3 + e$$

IO_3^- photodetaches an electron to produce neutral IO_3.
Other possible products are

$$IO_3 + hv \rightarrow IO_2^- + O(^1D)$$
$$\rightarrow IO_2 + O^-(^2P)$$
$$\rightarrow IO_2^- + O(^3P)$$

Depending on the absorption energy, the above channels are plausible, since, there is high density of electronic states of the IO_3^- (for hv < 263 nm) and these states cross the ground state of the neutral which easily lead to photodetachment.

Mechanism 2

IO_3^- is characterized by many excited stable states and present real minimum in their PES (their minimum located below the ground state of the neutral and correlate to dissociation limits located below the first dissociation limit of the neutral, Fig S1). Absorption of a photon in visible or near UV region i.e. (263 < hv < 442 nm) to these states may lead to the production of IO_2^- +O. Indeed, three triplet states correlate to the first dissociation limit, and these states are crossed by singlet states that correlates to IO_2+O^- dissociation limit. In this case, the photodissociation process may occur through the spin-orbit coupling at the crossing point between singlet-triplet to produce IO_2^- and O in their ground electronic states.

Moreover, the first excited singlet state of IO_3^- is unstable relative to IO^- + O_2 dissociation limit. Since the minimum of S_1 located above the IO^- + O_2 dissociation limit and absorption to S1 state may lead to IO^- + O_2 product and this competes with the production of IO_2^- +O and IO_3 + e.
The destruction of IO_3^- easily occurs for shorter wavelength whereas its photodissociation for longer wavelength is less plausible since the lowest singlet and triplet state are weakly bounded and their minimum located below the first dissociation limits.

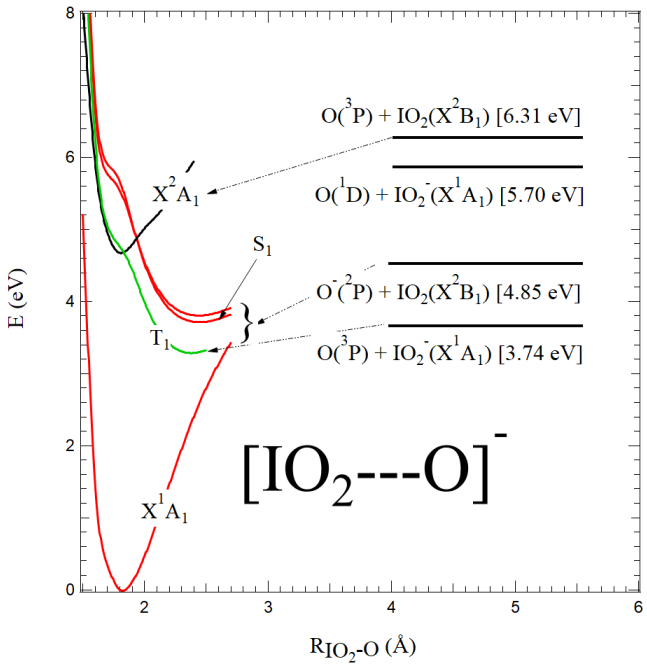

Fig S1. MRCI+Q/aug-cc-pVTZ-PP PES of the low-lying excited state of IO_3^- along the IO bond length. The electronic ground state of the neutral IO_3 is shown in black. Default active space selected for all calculations at MRCI+Q level.

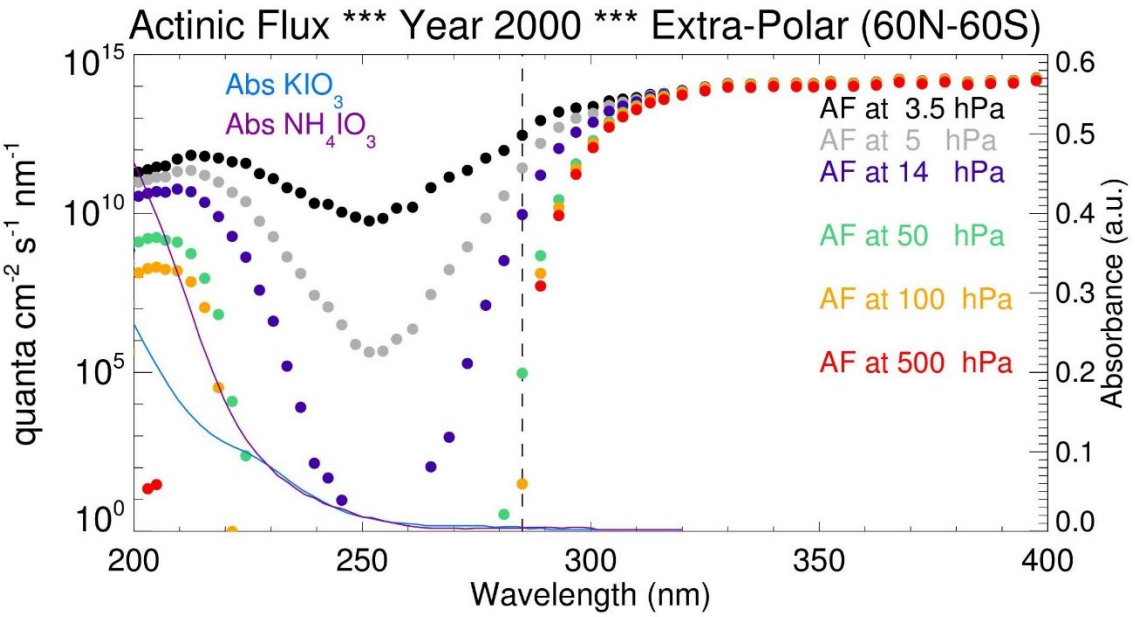

Figure S2. Modeled 2000 annual averaged wavelength dependent Actinic flux (AF) at different altitudes, together with the absorbance of iodate (KIO_3 and NH_4IO_3) species from Galvez et al., 2016(2).

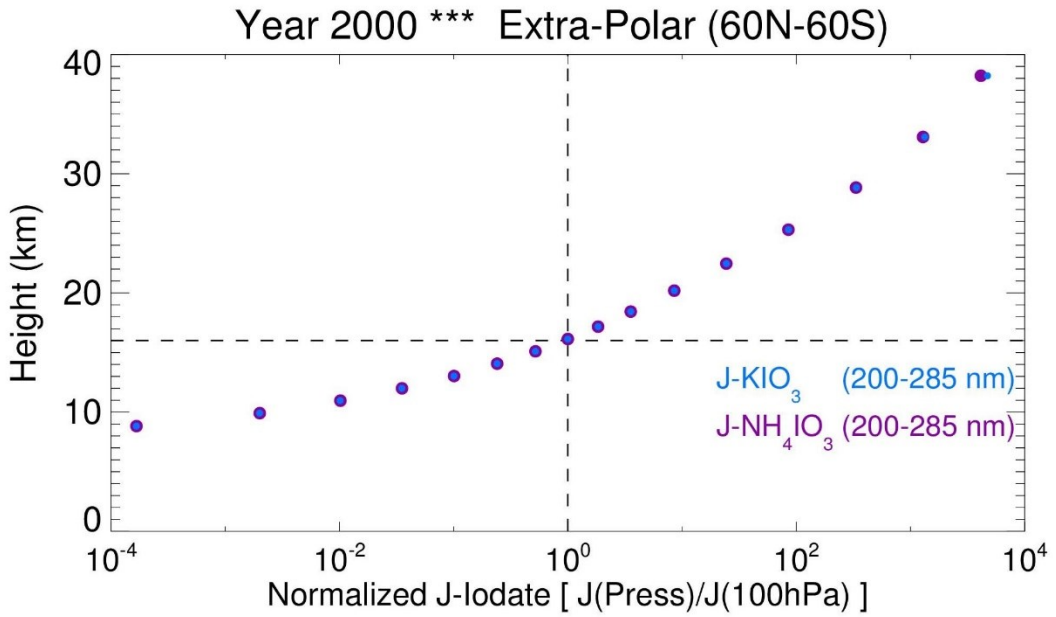

Figure S3. Vertical profile of normalized iodate (KIO_3 and NH_4IO_3) photolysis rates averaged during year 2000 within the extra-polar (60ºS-60ºN) region. J-iodate normalization has been performed with respect to the J-value obtained at approx. 100 hPa (~16-17 km). The wavelength range used for the photolysis rate computation is 200-285 nm (Fig. S2).

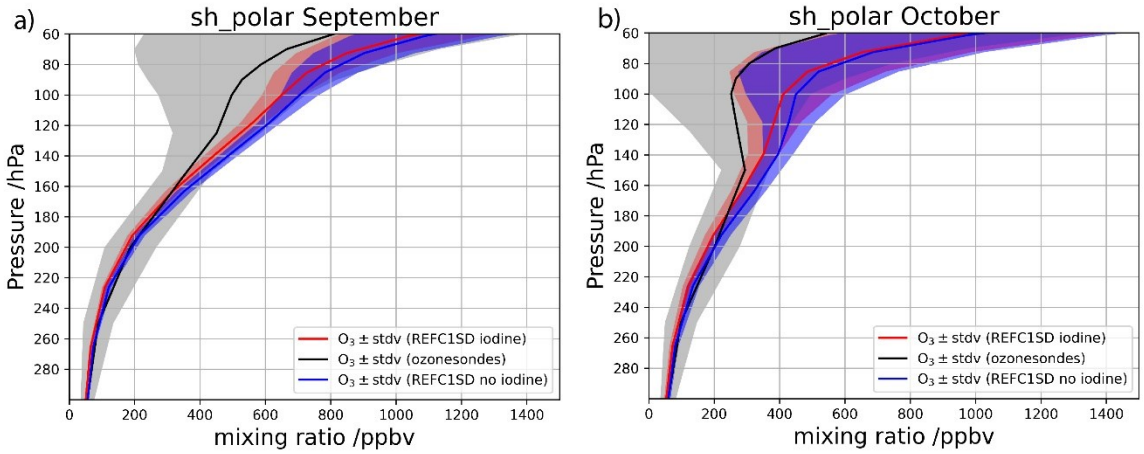

Figure S4. Comparison of model output (from base iodine and without iodine simulations) to ozonesonde climatology between 1995 and 2011 for the months of September and October. Observations from (3)

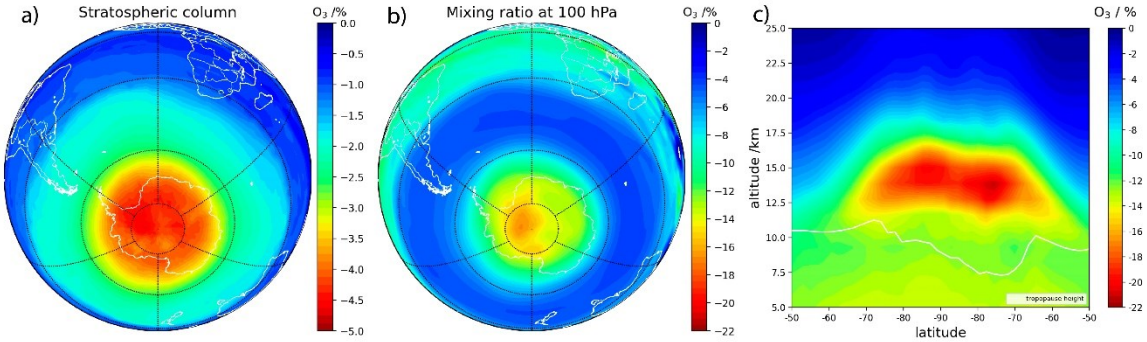

Figure S5. Effect of iodine chemistry in the Antarctic stratospheric ozone depletion in September 1993: a) effect on the stratospheric vertical column, b) effect at 16 km altitude (~100 hPa) and c) averaged meridional slice at 0º longitude, in which the effect of iodine chemistry can be seen spatially as a function of latitude and altitude. The relative percentage difference has been computed as ((iodine run – no iodine run) / no iodine run) × 100.

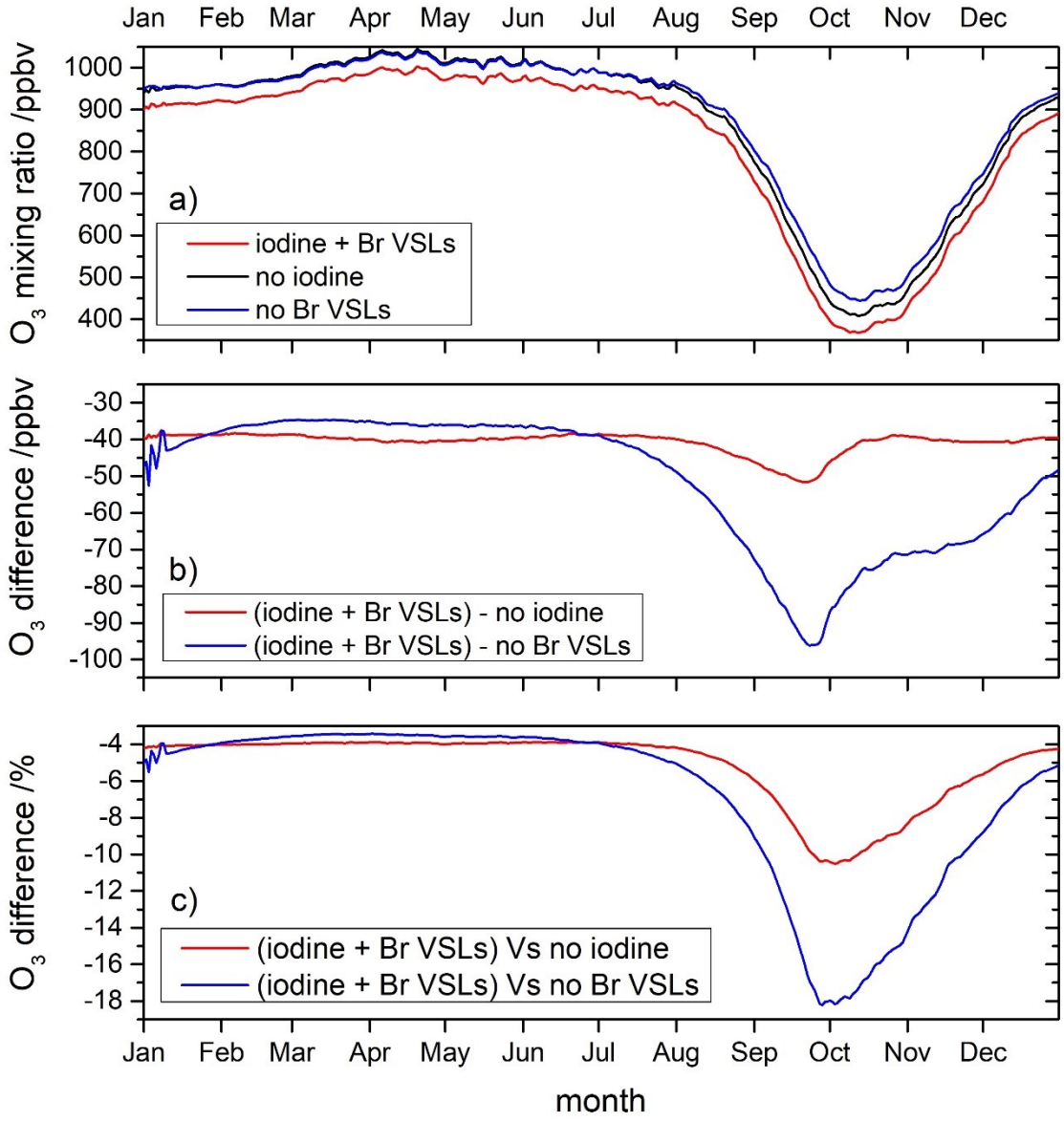

Figure S6. Daily evolution of the ozone hole during the 1980-2015 period in the region 90ºS-70ºS at 13-17 km altitude for the three simulations (a). The iodine run includes the three halogen chemical scheme (red line), the no iodine run includes only bromine and chlorine (black line), and the no Br VSLs run includes only iodine and chlorine VSLs (blue line). b) shows the ozone absolute difference in ppbv between the iodine and the no iodine runs and the difference between the iodine and no Br VSLs run. c) is the same as b) but displaying the ozone difference in percentage.

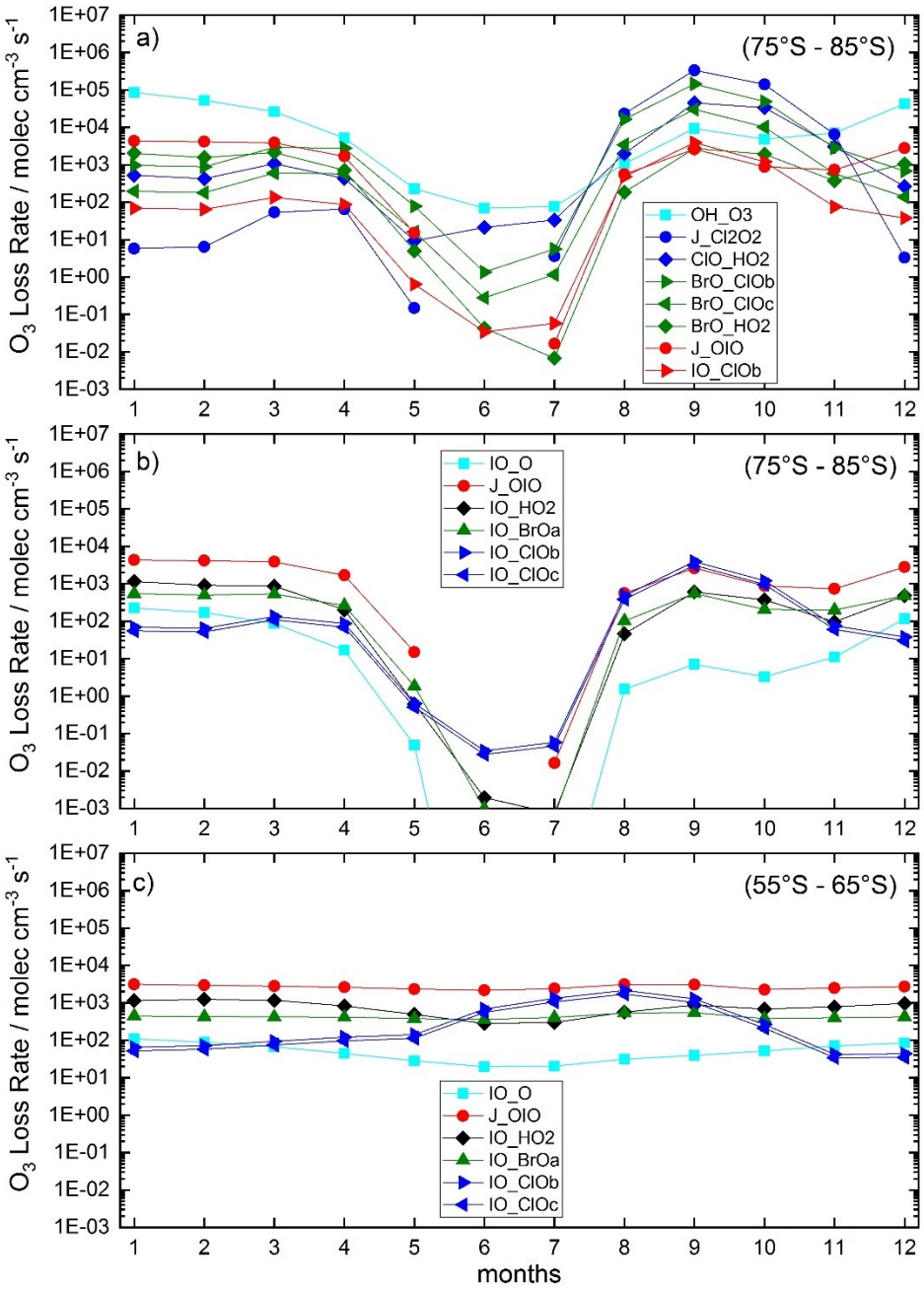

Figure S7: Absolute ozone loss rates averaged in the 85ºS-75ºS region at an altitude of 16 km (100 hPa). a) main loss rates for each family (grouped in colors) during spring for the simulation with iodine (filled symbols) and the simulation without iodine run (Empty symbols); b) ozone loss rates by iodine; c) is the same as a) for mid-latitudes (65ºS-55ºS). J(OIO) is the main channel in both regions, although inside the polar vortex this channel is matched by IO_ClO during spring. Outside the polar vortex the second channel is IO_HO2, followed by IO_BrO. Only during wintertime, the IO_ClO channels become more important but never exceed the J(OIO) channel.

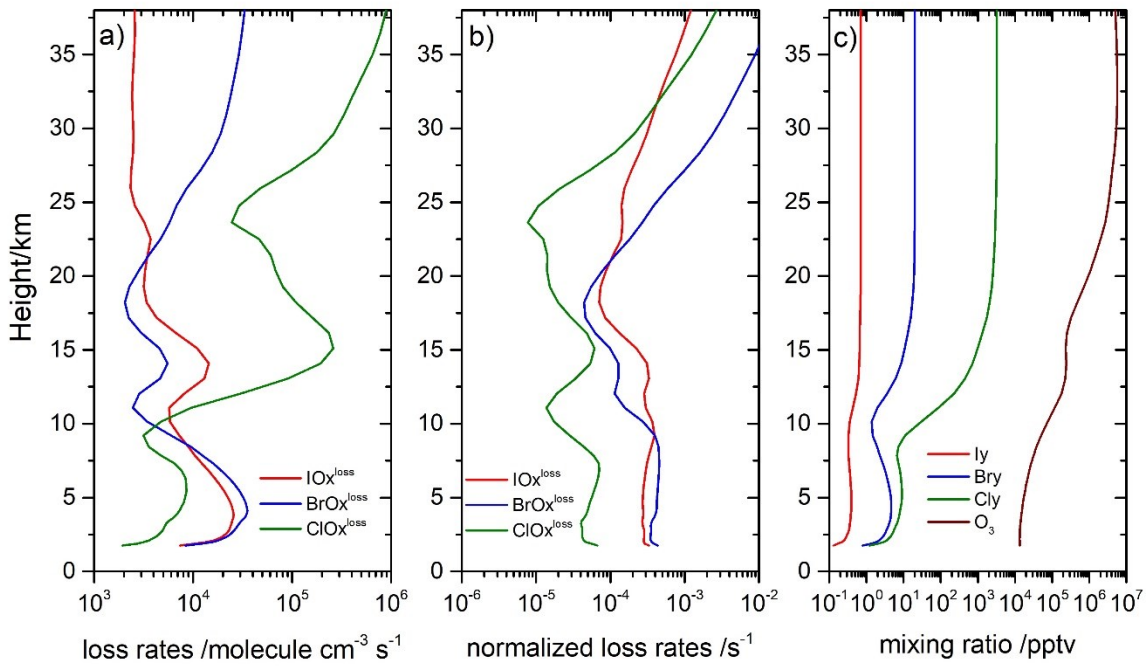

Figure S8. Absolute ozone loss rates for the three families $BrOx^{loss}$, $ClOx^{loss}$ and IOx^{loss} (a), ozone loss rates for the three halogen families normalized to Br_y, Cl_y and I_y concentrations (b), and vertical profile of I_y, Br_y and Cl_y and ozone (c). The data in this figure are results for mean October 2007 output averaged in the region 90ºS-70ºS at 13-17 km altitude from the simulation with iodine. Note: in the middle panel, ozone loss rates for I_x have been normalized to I_y+Br_y mixing ratios.

	CASSCF/aug-cc-pVTZ		MRCI+Q/aug-cc-pVTZ	
	Ev(nm)	Ead (nm)	Ev(nm)	Ead (nm)
S0	--	--	--	
T1	285	516	**259**	**490***
T2	262		258	
S1	240	427	**225**	**442***
S2	239		220	

**Not corrected with ZPE*

Table S1: Adiabatic (E_{ad}) and vertical (Ev) excitation energies in nm

Ground state S_0 (MRCI/USERDEF ENERGY=-520.10916268)			
I	0.4255210134	-0.2373158700	-0.3727807612
O	-0.4151984781	1.2188623569	0.3242599813
O	2.1070035827	-0.2373158700	0.3242607988
O	-0.4151984781	-1.6934940969	0.3242599813
First excited state S1 (MRCI/USERDEF ENERGY=-520.00593233)			
I	0.4255204022	-0.2373158700	0.0434215365
O	-0.5313697158	1.4200706520	0.1855258269
O	2.3393466693	-0.2373158700	0.1855268097
O	-0.5313697157	-1.8947023919	0.1855258269
First triplet state T1 (MRCI/USERDEF ENERGY=-520.01590078)			
I	0.4255040992	-0.2373986019	0.1068690058
O	-0.4858157770	1.3412221630	0.1565547973
O	2.2482541634	-0.2372888314	0.1593931470
O	-0.4858148455	-1.8157982095	0.1631130500

Table S2: XYZ coordinates at MRCI+Q/aug-cc-pVTZ-PP

IO_3^-(CASSCF/aug-cc-pVTZ)							
	ω_1	ω_2	ω_3	ω_4	ω_5	ω_6	ZPE
S_0	795	795	748	326	278	278	1611
S_1	532	468	468	434	86	85	1038
S_2	1046	567	489	489	132	132	1428
T_1	552	504	504	256	31	31	908

Table S3: CASSCF/aug-cc-pVTZ harmonic vibrational frequencies (ω_i in cm^{-1}) of the low-lying electronic state of IO_3^-.

Reaction	Heterogeneous sulphate aerosol reactions	Reactive uptake
R1	$N_2O_5 + H_2O(l) \rightarrow 2HNO_3$	γ=f(wt%)
R2	$ClONO_2 + H_2O(l) \rightarrow HOCl + HNO_3$	γ=f(T, P, HCl, H_2O ,r)
R3	$BrONO_2 + H_2O(l) \rightarrow HOBr + HNO_3$	γ=f(T, P, H_2O ,r)
R4	$ClONO_2 + HCl(l) \rightarrow Cl_2 + HNO_3$	γ=f(T, P, HCl, H_2O ,r)
R5	$HOCL + HCl(l) \rightarrow Cl_2 + H_2O$	γ=f(T, P, HCl, HOCl, H_2O ,r)
R6	$HOBr + HCl(l) \rightarrow BrCl + H_2O$	γ=f(T, P, HCl, HOBr, H_2O ,r)
R7	$HOCL + HBr(l) \rightarrow BrCl + H_2O$	$\gamma=\gamma$(R6)
R8	$HOBr + HBr(l) \rightarrow Br_2 + H_2O$	$\gamma=\gamma$(R6)
R9	$HOCL + HI(l) \rightarrow ICl + H_2O$	$\gamma=\gamma$(R6)
R10	$HOBr + HI(l) \rightarrow IBr + H_2O$	$\gamma=\gamma$(R6)
R11	$IONO_2 + H_2O(l) \rightarrow HOI + HNO_3$	$\gamma=\gamma$(R3)
R12	$HOI + HCl(l) \rightarrow ICl + H_2O$	$\gamma=\gamma$(R6)
R13	$HOI + HBr(l) \rightarrow IBr + H_2O$	$\gamma=\gamma$(R6)
R14	$HOI + HI(l) \rightarrow I_2 + H_2O$	$\gamma=\gamma$(R6)
	Nitric Acid Di-hydrate reactions	
R15	$N_2O_5 + H_2O(s) \rightarrow 2HNO_3$	γ=0.0004, JPL10-6
R16	$ClONO_2 + H_2O(s) \rightarrow HOCl + HNO_3$	γ=0.004, JPL10-6
R17	$ClONO_2 + HCl(s) \rightarrow Cl_2 + HNO_3$	γ=0.2, JPL10-6
R18	$HOCl + HCl(s) \rightarrow Cl_2 + H_2O$	γ=0.1, JPL10-6
R19	$HOBr + HCl(s) \rightarrow BrCl + H_2O$	$\gamma=\gamma$(R18)
R20	$HOCl + HBr(s) \rightarrow BrCl + H_2O$	$\gamma=\gamma$(R18)
R21	$HOBr + HBr(s) \rightarrow Br_2 + H_2O$	$\gamma=\gamma$(R18)
R22	$HOCl + HI(s) \rightarrow ICl + H_2O$	$\gamma=\gamma$(R18)
R23	$HOBr + HI(s) \rightarrow IBr + H_2O$	$\gamma=\gamma$(R18)
R24	$BrONO_2 + H_2O(s) \rightarrow HOBr + HNO_3$	γ=0.006 Davies et al., 2003
R25	$IONO_2 + H_2O(s) \rightarrow HOI + HNO_3$	$\gamma=\gamma$(R24)
R26	$HOI + HCl(s) \rightarrow ICl + H_2O$	$\gamma=\gamma$(R18)
R27	$HOI + HBr(s) \rightarrow IBr + H_2O$	$\gamma=\gamma$(R18)
R28	$HOI + HI(s) \rightarrow I_2 + H_2O$	$\gamma=\gamma$(R18)
	Ice aerosol reaction	
R29	$N_2O_5 + H_2O(s) \rightarrow 2HNO_3$	γ=0.02, JPL10-6
R30	$ClONO_2 + H_2O(s) \rightarrow HOCl + HNO_3$	γ=0.3, JPL10-6
R31	$BrONO_2 + H_2O(s) \rightarrow HOBr + HNO_3$	γ=0.3, JPL10-6
R32	$ClONO_2 + HCl(s) \rightarrow Cl_2 + HNO_3$	γ=0.3, JPL10-6
R33	$HOCl + HCl(s) \rightarrow Cl_2 + H_2O$	γ=0.2, JPL10-6
R34	$HOBr + HCl(s) \rightarrow BrCl + H_2O$	γ=0.3, JPL10-6
R35	$HOCl + HBr(s) \rightarrow BrCl + H_2O$	$\gamma=\gamma$(R33)
R36	$HOBr + HBr(s) \rightarrow Br_2 + H_2O$	$\gamma=\gamma$(R34)
R37	$HOCl + HI(s) \rightarrow ICl + H_2O$	$\gamma=\gamma$(R33)
R38	$HOBr + HI(s) \rightarrow IBr + H_2O$	$\gamma=\gamma$(R33)
R39	$IONO_2 + H_2O(s) \rightarrow HOI + HNO_3$	$\gamma=\gamma$(R31)
R40	$HOI + HCl(s) \rightarrow ICl + H_2O$	$\gamma=\gamma$(R34)
R41	$HOI + HBr(s) \rightarrow IBr + H_2O$	$\gamma=\gamma$(R34
R42	$HOI + HI(s) \rightarrow I_2 + H_2O$	$\gamma=\gamma$(R34)
R43	$HOI + HCl(s) \rightarrow ICl + H_2O$	$\gamma=\gamma$(R34)

Table S4. Summary of stratospheric heterogeneous bromine, chlorine and iodine reactions on sulfate, NAT and ice aerosols considered in WACCM4. Uptake coefficients (γ) for iodine reactions have been mapped to their equivalent reactions for bromine. Reactions highlighted in blue are the additional heterogeneous iodine reactions with respect to the standard WACCM scheme.

SI References

1. H. Wen, G.-L. Hou, W. Huang, N. Govind, X.-B. Wang, Photoelectron spectroscopy of higher bromine and iodine oxide anions: Electron affinities and electronic structures of BrO2,3 and IO2–4 radicals. *J. Chem. Phys.* **135**, 184309 (2011).

2. Ó. Gálvez, M. T. Baeza-Romero, M. Sanz, A. Saiz-Lopez, Photolysis of frozen iodate salts as a source of active iodine in the polar environment. *Atmos. Chem. Phys.* **16**, 12703–12713 (2016).

3. S. Tilmes, *et al.*, Technical Note: Ozonesonde climatology between 1995 and 2011: description, evaluation and applications. *Atmos. Chem. Phys.* **12**, 7475–7497 (2012).